Global and Planetary Change 240 (2024) 104532

Contents lists available at ScienceDirect

Global and Planetary Change

journal homepage: www.elsevier.com/locate/gloplacha

Planktonic foraminifera response to the azores high and industrial-era global warming in the central-western Mediterranean Sea

Serena Ferraro [a], Alessandro Incarbona [b,c,*], Sergio Bonomo [a], Lucilla Capotondi [d], Luigi Giaramita [a], Leonardo Langone [e], Nereo Preto [f], Giovanni Surdi [b,c], Elena Zanola [f], Giorgio Tranchida [g]

[a] *Istituto di Geologia Ambientale e Geoingegneria, Consiglio Nazionale delle Ricerche (IGAG), Area Della Ricerca di Roma 1- Strada Provinciale 35d, Montelibretti 9-00010, RM, Italy*
[b] *Università degli Studi di Palermo, Dipartimento di Scienze della Terra e del Mare, Via Archirafi 22, 90134 Palermo, Italy*
[c] *National Biodiversity Future Center (NBFC), Palermo 90133, Italy*
[d] *Istituto per le Scienze Marine, Consiglio Nazionale delle Ricerche (ISMAR), Via Gobetti 101, 40129 Bologna, Italy*
[e] *Istituto per le Scienze Polari, Consiglio Nazionale delle Ricerche (ISP), Via Gobetti 101, 40129 Bologna, Italy*
[f] *Dipartimento di Geoscienze, Università degli Studi di Padova, Via G. Gradenigo 6, 35131 Padova, Italy*
[g] *Istituto per lo studio degli impatti Antropici e Sostenibilità in ambiente marino, Consiglio Nazionale delle Ricerche (IAS-CNR), Via Del Mare 3, 91021 Torretta Granitola fraz, Campobello di Mazara (TP), Italy*

ARTICLE INFO

Editor: Fabienne Marret-Davies

Keywords:
Biodiversity
Productivity
Calcareous plankton
Climate change
Sicily channel

ABSTRACT

The Mediterranean Sea is warming about 20 % more rapidly than global ocean and this phenomenon is impacting ecosystems and biodiversity. Planktonic foraminifera are an important component of surface and subsurface water ecosystems and food chains. Their species communities have been altering across the oceans since the Industrial Era, in response to the ongoing climate change, especially in the western Mediterranean Sea, where a significant productivity decrease has been recently reported.

Here we show planktonic foraminifera and multispecies stable isotopes from three short sediment cores, recovered on the eastern flank of the Sicily Channel, central Mediterranean Sea. Results fully confirm the planktonic foraminifera productivity decrease in the Industrial Era, which is especially relevant for the second half of the 20th century. The planktonic foraminifera productivity decrease matches with a higher number of Large Azores High events, *i.e.*, the establishment of an exceptional and persistent winter atmospheric high-pressure ridge over the western-central Mediterranean Sea. This is an unprecedented atmospheric phenomenon for the last millennia Mediterranean Sea history, as a direct response of the global warming. Surface productivity and DCM species are especially declining since ~1960 CE, at expenses of winter mixed layer taxa, suggesting that the Azores High activity prevents a sustained water column vertical mixing and surface water nutrient fuelling. Our results document and confirm that the climate change has already been affecting Mediterranean marine ecosystems and the basic level of the trophic chain, by extending the surface water stratification period.

1. Introduction

The Mediterranean Sea is thought to be a climate change hotspot (Giorgi and Lionello, 2008). Combined instrumental and proxy data for sea surface temperatures (SSTs) show that since the second half of the 19th century, Mediterranean SSTs have increased by ~1.54 °C ± 0.09 °C at an average warming rate of 0.33 °C per decade (Marriner et al., 2022), about 20 % more than global ocean on average (MedECC, 2021). Many reports clearly establish a thorough impact of SST warming and increased frequency of marine heat waves on ecosystems and biodiversity (MedECC, 2021). However, ecological studies and instrumental time series can only give a snapshot of the modern environmental framework and do not fully cover the anthropogenic perturbation, started in 1857 Common Era (CE), with the second industrial revolution. A longer time perspective is needed to assess the starting point of biodiversity and ecosystems alteration, based on the

* Corresponding author at: Università degli Studi di Palermo, Dipartimento di Scienze della Terra e del Mare, Via Archirafi 22, 90134 Palermo, Italy.
E-mail address: alessandro.incarbona@unipa.it (A. Incarbona).

https://doi.org/10.1016/j.gloplacha.2024.104532
Received 2 February 2024; Received in revised form 18 June 2024; Accepted 24 July 2024
Available online 27 July 2024

investigation of marine sediments and proxy data.

Planktonic foraminifera are unicellular zooplankton organisms, widely adopted for palaeoenvironmental reconstructions (e.g. Schiebel and Hemleben, 2017). They proved to be sensitive to the ongoing climate change, because species communities across the oceans are altered since the Industrial Era (Jonkers et al., 2019). Over the last two kiloyears (kyr), many studies show that Mediterranean Sea planktonic foraminifera assemblages were modified by different factors including hydrological, climatic and also anthropogenic forcing (Pallacks et al., 2021; Incarbona et al., 2019; Lirer et al., 2013; Margaritelli et al., 2016, 2018; Vallefuoco et al., 2012). Importantly, a decrease in planktonic foraminifera accumulation rate in the Alboran and Balearic Seas has been reported since the Industrial Era (IE), likely induced by local enhanced vertical stratification (Pallacks et al., 2021). The composition of planktonic foraminifera from surface sediments provides a snapshot of modern Mediterranean assemblages (Azibeiro et al., 2023; Kontakiotis et al., 2021; Zarkogiannis et al., 2020). A very recent report suggests that they are mainly controlled by hydrology and vertical water column dynamics, rather than by SST change alone (Azibeiro et al., 2023).

Here we show planktonic foraminiferal abundance and accumulation rates from three sedimentary cores recovered in the Sicily Channel, along a N-S transect, over the last three kyr and compare them to those collected in the central-western Mediterranean Sea (Incarbona et al., 2019; Margaritelli et al., 2018; Margaritelli et al., 2016; Pallacks et al., 2021; Vallefuoco et al., 2012). Such a dense spatial coverage allows us to shape planktonic foraminiferal assemblage variations between the pre-industrial and industrial Era, in a region subjected to multiple hydrological and atmospheric forcings (Incarbona et al., 2016; Incarbona et al., 2013).

2. Living planktonic foraminiferal surveys

Strong oligotrophy in the Mediterranean Sea is maintained by the anti-estuarine circulation pattern, since outflow of nutrient-enriched intermediate water (LIW) is replaced by inflow of nutrient-depleted surface water (MAW) (Béthoux, 1979; Sarmiento et al., 1988). Winter convection, frontal zones and coastal upwelling may occasionally bring LIW into the photic zone, providing nutrients for fertilization in the upper part of the water column (Krom et al., 2010). In summer, a deep stable stratification takes place, hindering nutrient uplift (Allen et al., 2002; Klein and Coste, 1984). In the Sicily Channel, about 80% of primary productivity variance are explained by the advection of chlorophyll and nutrients in MAW from the North African coast (Rinaldi et al., 2014). These described features strongly affect the marine biota, like foraminiferal communities.

Vicomed I summer (September-October 1986) and Vicomed II winter (February-March 1988) cruises provide the most complete documentation on living planktonic foraminifera throughout the Mediterranean Sea (Pujol and Vergnaud Grazzini, 1995). In this marginal basin, the living foraminiferal species are mainly related to the regional hydrographic patterns. Hydrography controls the seasonality and depth of the turbulent mixing (which differs between the western and the eastern Basins), the depth of the mixed layer and its seasonal stratification, as well the strength of the pycnocline (Pujol and Vergnaud Grazzini, 1995).

Fig. 2 highlights the highest abundance of planktonic foraminifera in the western basin in winter, whereas summer productivity is prevalent in the eastern Mediterranean. Two stations were sampled at western and eastern sills of the Sicily Channel (Fig. 1). The productivity regime of both sites shows transitional features of the two basins: the number of individuals is still relatively high, somewhat comparable to Algerian and Sardinia sites, but with prevalent summer productivity like eastern settings (Fig. 2). The most peculiar feature of the Sicily Channel planktonic foraminiferal assemblages is the very high abundance of *Globigerinoides ruber* pink (almost 90% at the western entrance in summer) (Pujol and Vergnaud Grazzini, 1995). This dominance is not

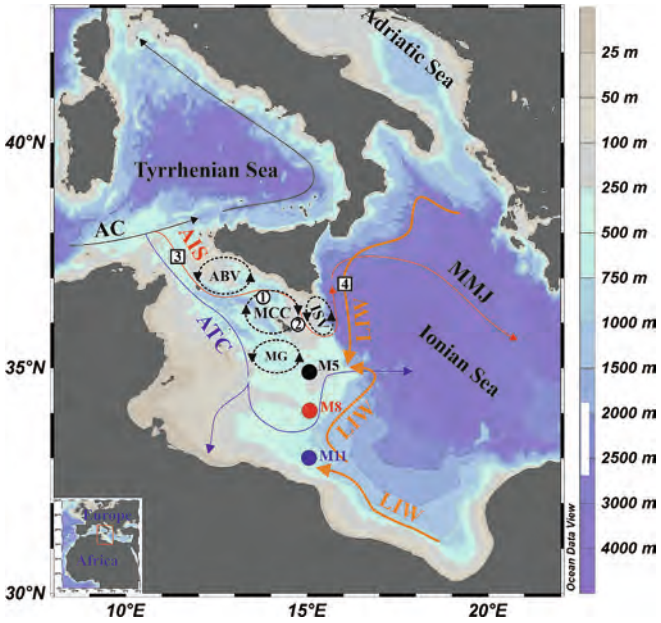

Fig. 1. Bathymetric map of the central Mediterranean Sea (Ocean Data View software) and location map of M5, M8 and M11 cores (respectively black, red and blue circles). Oceanographic features are modified from Pinardi and Masetti (2000). Black, blue and red arrows show the MAW path: AC, Algerian Current; AIS, Atlantic Ionian Stream; ATC, Atlantic Tunisian Current; MMJ, Mid-Mediterranean Jet. Dashed line black arrows show semipermanent mesoscale summer features: ABV, Adventure Bank Vortex cyclonic gyre; MCC, Maltese Crest Channel anticyclonic gyre; ISV, Ionian Shelfbreak Vortex cyclonic gyre; MG, Medina cyclonic Gyre. Orange arrows show the LIW path. Circles 1 and 2 show St 342 and St 407 cores (Incarbona et al., 2019). Squares 3 and 4 show stations of the coccolithophore surveys VICOMED I and II (Pujol and Vergnaud Grazzini, 1995). (For interpretation of the references to colour in this figure legend, the reader is referred to the web version of this article.)

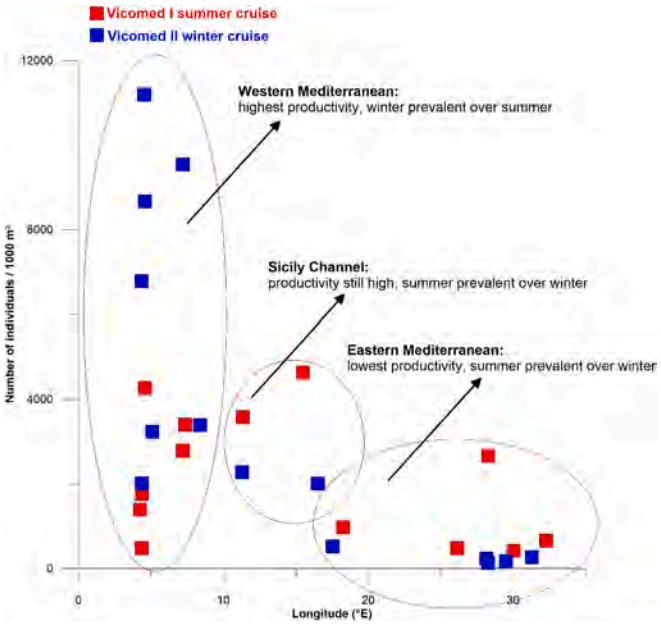

Fig. 2. Plot between the number of planktonic foraminiferal individuals on 1000 m^3 and the longitude (°E), as recovered in the Mediterranean summer and winter VICOMED I and II cruises (Pujol and Vergnaud Grazzini, 1995). Western Mediterranean, Sicily Channel and eastern Mediterranean productivity styles are briefly commented.

further observed in the ABV area in spring 2013, when indeed *G. ruber* pink was very rare (Mallo et al., 2017). During Vicomed II winter cruise, *Globigerina bulloides*, *Globorotalia inflata* and *Globorotalia truncatulinoides* were significantly abundant (Pujol and Vergnaud Grazzini, 1995). Looking at species distribution in the surface sediments, the Malta Escarpment where our N-S transect of cores was recovered, a major turning point between the western and eastern Mediterranean Sea is here observed. Relatively high *G. ruber* and low *G. bulloides*, *G. inflata* and *G. truncatulinoides* abundances denote a greater affinity for eastern Mediterranean assemblages, as observed in the distribution maps of major species (Azibeiro et al., 2023; Kontakiotis et al., 2021).

3. Planktonic foraminiferal ecological preferences

Globigerinoides ruber pink and white thrive in warm, stratified and oligotrophic water. A distinct preference of *G. ruber* pink for late summer months is often observed (Morard et al., 2019; Pujol and Vergnaud Grazzini, 1995; Richey et al., 2019; Rigual-Hernández et al., 2012; Schiebel and Hemleben, 2017; Žarić et al., 2005). Ecological studies on modern *G. ruber* from plankton tows in the Mediterranean Sea document that this species dominates planktonic foraminifera assemblages during late summer in the western basin and throughout the year in the eastern basin (Giamali et al., 2021; Giamali et al., 2020; Kontakiotis et al., 2021; Mallo et al., 2017; Pujol and Vergnaud Grazzini, 1995).

Globigerina bulloides is a proxy for cold upwelled water, like in eutrophic waters (Peeters et al., 2002; Schiebel and Hemleben, 2017). In the Mediterranean Sea, *G. bulloides* proliferates in productive surface water due to winter vertical mixing or frontal areas (Pujol and Vergnaud Grazzini, 1995; Rigual-Hernández et al., 2012). *Globorotalia inflata* is associated with hydrologic fronts and eddies and with coastal upwelling (Pujol and Vergnaud Grazzini, 1995; Schiebel and Hemleben, 2017). *Globorotalia truncatulinoides* is a deep dwelling species, a proxy for a deep winter mixed layer (Margaritelli et al., 2022; Margaritelli et al., 2020; Pujol and Vergnaud Grazzini, 1995; Schiebel and Hemleben, 2017). *Neogloboquadrina incompta* exhibits a preference for a deep chlorophyll maximum (Fairbanks and Wiebe, 1980; Pujol and Vergnaud Grazzini, 1995). In the Mediterranean Sea, *N. incompta* is significantly abundant in the Gulf of Lions region, where it peaks in winter-spring (Azibeiro et al., 2023; Rigual-Hernández et al., 2012). *Globigerinella siphonifera* is common and abundant in tropical and subtropical oceans (Schiebel and Hemleben, 2017). *Globigerinella calida* belongs to the *G. siphonifera plexus*, with which it shares the same geographical distribution (Schiebel and Hemleben, 2017). *Orbulina universa* is abundant from tropical to temperate waters and tolerates a wide range of water salinity and temperature (Bijma et al., 1990; Schiebel and Hemleben, 2017). *Trilobatus trilobus* group species thrive in low-salinity tropical and subtropical warm oligotrophic surface water (Checa et al., 2020; Jonkers and Kučera, 2015; Pujol and Vergnaud Grazzini, 1995; Sprovieri et al., 2003; Zarkogiannis et al., 2020). *Globoturborotalita rubescens* thrives in tropical to temperate surface water (Schiebel and Hemleben, 2017; Seears et al., 2012) In the Mediterranean Sea, it is more abundant in the Ionian Sea and in the far eastern Mediterranean (Azibeiro et al., 2023). *Turborotalita quinqueloba* prefers cold and high fertility surface water (Incarbona et al., 2013; Schiebel and Hemleben, 2017; Sprovieri et al., 2003). *Globigerinita glutinata* is a temperate and cold-water species that increases in response to phytoplankton blooming (Jonkers and Kučera, 2015; Schiebel and Hemleben, 2005; Schmuker and Schiebel, 2002). *Globigerinoides conglobatus* dwells in the deeper photic zone of tropical and subtropical water (Schiebel and Hemleben, 2005). In present day Mediterranean Sea, it is very rarely found (Azibeiro et al., 2023; Pujol and Vergnaud Grazzini, 1995).

4. Study area

4.1. Hydrological and atmospheric framework

The Mediterranean anti-estuarine circulation pattern is forced by its negative hydrological balance (Robinson and Golnaraghi, 1994), which is matched by Atlantic Ocean surface water. The Mediterranean thermohaline circulation mirrors global ocean processes, albeit on the smaller temporal and spatial scale (Bethoux et al., 1999). Surface water from the Atlantic Ocean (Modified Atlantic Water - MAW) splits into two streams at the entrance of the Sicily Channel (Béranger et al., 2004; Pinardi and Masetti, 2000; POEM group, 1992; Robinson et al., 1999): the Atlantic Tunisian Current (ATC) flows eastwards, along the African coast, and is prevalent in winter (Fig. 1); the northern branch, the Atlantic Ionian Stream (AIS), feeds the Mid-Mediterranean Jet that flows eastward up to the Levantine basin and is prevalent in summer (Fig. 1).

Three semipermanent meso-scale summer features are associated with AIS meanders in southern Sicily offshore, the Adventure Bank Vortex cyclonic gyre, the Maltese Crest Channel anticyclonic gyre and the Ionian Shelfbreak Vortex cyclonic gyre (Fig. 1) (Béranger et al., 2004; Lermusiaux and Robinson, 2001; Onken, 2003). A further semipermanent meso-scale cyclonic gyre, the Medina cyclonic Gyre, occur south of Malta (Fig. 1) (Jouini et al., 2016; Menna et al., 2019). These meso-scale features vary in size, strength and interact with each other, determining different seasonal water column dynamics and productivity modes (Béranger et al., 2004; Lermusiaux and Robinson, 2001).

A severe salt-enrichment leads to Levantine Intermediate Water (LIW) formation in winter, in an area between Rhodes and Cyprus islands (Malanotte-Rizzoli and Hecht, 1988; POEM group, 1992). LIW occupies a layer between 150 and 200 and 600 m water depth and enters the Sicily Channel through the sills south of Malta (Fig. 1), occasionally together with a thin thickness of the uppermost layer of Eastern Mediterranean Deep Water (Gasparini et al., 2005; Lermusiaux and Robinson, 2001).

Seasonal atmospheric variations in the Mediterranean/European region are controlled by the transition between the subtropical high-pressure belt over North Africa and westerlies over central and western Europe. The latitudinal shift of the transition between the subtropical high-pressure belt over North Africa and westerlies over central and western Europe brings about drought or penetration of Atlantic low-pressure areas respectively in summer and winter (Rohling et al., 2015). The North Atlantic Oscillation (NAO) largely controls rainfall patterns over the Mediterranean region. Wet westerlies blow across northern Europe during positive NAO-index phases and dry conditions are established in southern Europe and northern Africa, while the hydrological pattern is reversed during negative NAO-index phases (Comas-Bru and McDermott, 2014). Other indices, such as the Mediterranean Oscillation Index, are important for describing local rainfall patterns, but are usually linked to large-scale atmospheric circulation dynamics, primarily to the NAO (Lionello, 2012).

The Atlantic Multidecadal Oscillation (AMO), defined by detrended SST anomalies averaged over the North Atlantic from 0° to 70°N (Enfield et al., 2001), is correlated with Mediterranean SSTs of the last 150 years (Marullo et al., 2011). Other multidecadal atmospheric patterns, like Eastern Atlantic or Eastern Atlantic/Western Russian (EA/WR) may impact northern borderlands surface heat exchanges and eastern Mediterranean deep-water production (Josey et al., 2011).

5. Material

M5 (15°10.62′E; 35°07.20′N; 509 m water depth), M8 (15°09.05'; 33°59.69'; 488 m water depth) and M11 (15°07.48'; 32°52.19'; 724 m water depth) short sediment cores were recovered by a multicorer on the eastern flank of the Sicily Channel in July 2010, during the MedSudMed'10 cruise (R/V Urania) (Fig. 1). They are respectively 17, 15 and 14-cm long. The sediment consists of fairly homogeneous light

brown silt and silty clays, devoid of visible bioturbation or macroscopic remains of organisms.

6. Methods

6.1. Planktonic foraminiferal analysis

A total of 17, 15 and 14 samples (spaced every 1 cm) for respectively M5, M8 and M11cores were considered for planktonic foraminiferal analysis. Samples were washed using a 63 μm mesh sieve and then oven-dried at 40 °C. Quantitative planktonic foraminiferal analysis was carried out on split aliquots containing over 300 specimens from the fraction >125 μm. Specimens were identified to the species level (21 species) following taxonomic concepts by Hemleben et al. (1989), Schiebel and Hemleben (2017) and Morard et al. (2019). The *Trilobatus trilobus* group includes *T. trilobus*, *Trilobatus sacculifer* and *Trilobatus quadrilobatus* (Spezzaferri et al., 2015).

The planktonic foraminiferal accumulation rates (number of specimens · cm^{-2} · kyr^{-1}) were calculated using the following equation:

planktonic foraminiferal concentration (number of specimens · g^{-1}) · sedimentation rate (cm · kyr^{-1}) dry bulk density (DBD) (g · cm^{-3}) (Pallacks et al., 2021).

The tropical/subtropical group includes *G. ruber* white, *G. ruber* pink, *G. siphonifera*, *G. calida*, *T. trilobus* group species, *G. rubescens*, *G. tenella* and *G. conglobatus*. The mixed layer group includes *G. inflata* and *G. truncatulinoides* and the surface productivity group includes *G. bulloides*, *G. glutinata*, *T. quinqueloba* and *G. scitula*. The Deep Chlorophyll Maximum (DCM) presence corresponds to the *N. incompta*. The *G. bulloides / G. bulloides + G. inflata + G. truncatulinoides* ratio indicates sea surface winter/spring productivity and a deep winter mixed layer or hydrological fronts, respectively for high and low values (Incarbona et al., 2019).

6.2. Stable isotopes

A total of 46 and 41 samples (every 1 cm, using the same samples of planktonic foraminifera analysis) were analyzed respectively for *G. ruber* white and *Uvigerina mediterranea* $\delta^{18}O$ and $\delta^{13}C$ in M5, M8 and M11. Analyses were carried out at the spectrometry laboratory of the Department of Geosciences University of Padova by an automated continuous flow carbonate preparation GasBench II device, attached to a Thermo Scientific Delta V Advantage Isotope Ratio Mass Spectrometer. Acidification of samples was performed at 70 °C. Every 7 samples, an internal standard (MAQ 1 with $\delta^{18}O$ = -1.15 ‰ and $\delta^{13}C$ = 2.58 ‰) was run for normalization, while 3 analyses of an internal quality assurance standard (GR 1 with $\delta^{18}O$ = -10.44 ‰ and $\delta^{13}C$ = 0.68 ‰) were ran for each batch of about 60 samples. In addition, a few repetitions of the international standards NBS 18 and NBS 19 were performed to ensure accuracy. External precision during the period of the analyses was better than 0.05 ‰ for $\delta^{13}C$ and better than 0.10 ‰ for $\delta^{18}O$, on the basis of repetitions of the quality assurance standard. All the isotope data are reported in δ ‰ *versus* VPDB.

6.3. ^{210}Pb radionuclides and radiocarbon datings

^{210}Pb activities were measured *via* alpha counting of its daughter, ^{210}Po, assuming secular equilibrium between the two isotopes. In M5, M8 and M11 cores, ^{210}Po was extracted from the sediment with hot HNO_3 and H_2O_2, after spiked with ^{209}Po (NIST standard SRM 4326, diluted to 0.43 Bq g^{-1}) used as a yield monitor. After separation of the leachate from the residue, the solution was evaporated to near dryness and the nitric acid was eliminated using concentrated HCl. The residue was dissolved in 1.5 N HCl. Iron was reduced using ascorbic acid and Po was plated onto a silver disk overnight, at room temperature (Frignani and Langone, 1991). The lowest values of total ^{210}Pb in the deepest part of cores were considered to estimate the value of the supported ^{210}Pb activity.

Three Accelerator Mass Spectrometry ^{14}C radiocarbon datings have been performed at CEDAD University of Salento, on about 0.25 g of mixed planktonic foraminiferal specimens, on the deepest sample of each core (M5, M8 and M11). Radiocarbon datings were calibrated by the curve Marine 13 (Reimer et al., 2013), with a $\Delta R = 0$ yr (Incarbona and Sprovieri, 2020).

7. Chronology

The chronological framework of each M5, M8 and M11 core is based on the combination of ^{210}Pb radionuclides and radiometric ages and their uncertainties were probabilistically assessed in a Bayesian deposition model by rbacon software version 2.5.8 (Blaauw and Christen, 2011).

^{210}Pb activity in the three cores is shown in in Supplementary Material 1 (SM1) Fig. S1, where it is evident that excess lead is limited to the top 4 cm in cores M5 and M8 and to the top 3 cm in core M11 (raw ^{210}Pb activity values are available in SM1 Table S1). Uncorrected radiocarbon datings are available in SM2 Table S2 and their calibration was automatically calculated by rbacon software version 2.5.8 (Blaauw and Christen, 2011) (Fig. 3). The rbacon software calibrations are identical to those achieved with OxCal 4.3.2, visible in SM2 Fig. S2.

The bayesian depth/age model of the three M5, M8 and M11 cores is shown in Fig. 3. It was assessed by combining ^{210}Pb based on Constant Flux: Constant Sedimentation (*CF*:CS) model and Bayesian models using bottom ^{14}C dates for each core.

Different sedimentation rates between the top (^{210}Pb activity) and the lower part (radiocarbon datings) of the cores may be overestimated, because of physical and chemical alterations in sediments, as commonly observed in other studies (Cisneros et al., 2016; Pallacks et al., 2021). The age uncertainty accuracy is especially verified for the top of the record, subjected to ^{210}Pb activity profiles (Pallacks et al., 2021), where we carried out most of our reasoning and discussion. The time resolution of this stratigraphic interval, which spans the last 100-150 years and covers the IE, is an average of 29, 22 and 28 years for respectively M5, M8 and M11 cores.

8. Results and discussion

8.1. Planktonic foraminifera

Globigerinoides ruber white is the dominant species in all M5, M8 and M11 cores (Fig. 4). Percentage abundance values in the different cores are linked to their latitudinal setting, being higher in the southernmost position (on average 37.6 % in core M5, 40.8 % in core M8 and 46.9 % in core M11), as already noted by Kontakiotis et al. (2021) and Zarkogiannis et al. (2020). A distinct abundance decline is observed since the passage from the Little Ice Age (LIA) to the IE (~ 1850 CE, Fig. 4). *Globigerinoides ruber* pink abundance distribution still shows the latitudinal effect but diverges from that one of the white subspecies because it increases since the IE (Fig. 4). Signals of modifications across the preindustrial/industrial Era are visible in different other species, especially since 1900-1950 CE, at least in two of the three cores (Figs. 4-6): abundance decreases in *G. bulloides*, *T. trilobus* and *G. rubescens*; abundance increases in *G. inflata*, *G. truncatulinoides* and *G. calida*. This supports the significant modification of planktonic foraminiferal assemblages since the IE, with a breakthrough in the twentieth century. We highlight that the most significant modern features in Sicily Channel planktonic foraminiferal assemblages, such as high abundances of *G. ruber* pink rather than *G. ruber* white or *G. inflata* rather than *G. bulloides* (Pujol and Vergnaud Grazzini, 1995), have been occurring since the beginning of the IE.

Little information is available in the interval before the IE, mostly because the relatively low-time resolution. The distribution pattern of each planktonic foraminiferal species is not always aligned among the

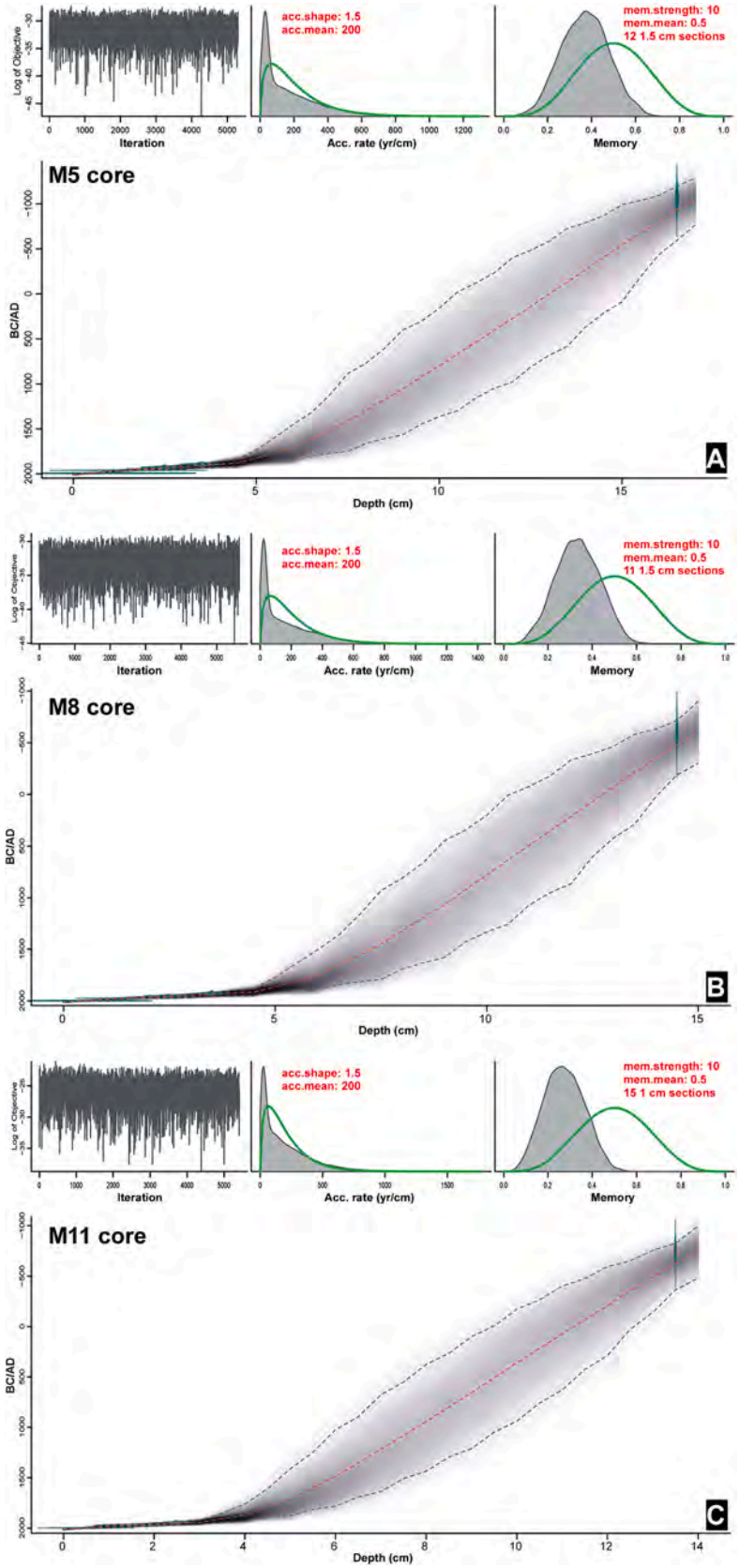

Fig. 3. Bayesian age models for M5 (A), M8 (B) and M11 (C) cores, assessed by calibrated ^{14}C and ^{210}Pb dates. The lower panel in A, B and C shows the depth/age plot, where dotted lines represent the 95% confidence interval. In the upper panels, from the left: Monte Carlo iterations; prior (green curve) and posterior (grey histogram) distribution of the accumulation rate; prior (green curve) and posterior (grey histogram) distribution of the memory. (For interpretation of the references to colour in this figure legend, the reader is referred to the web version of this article.)

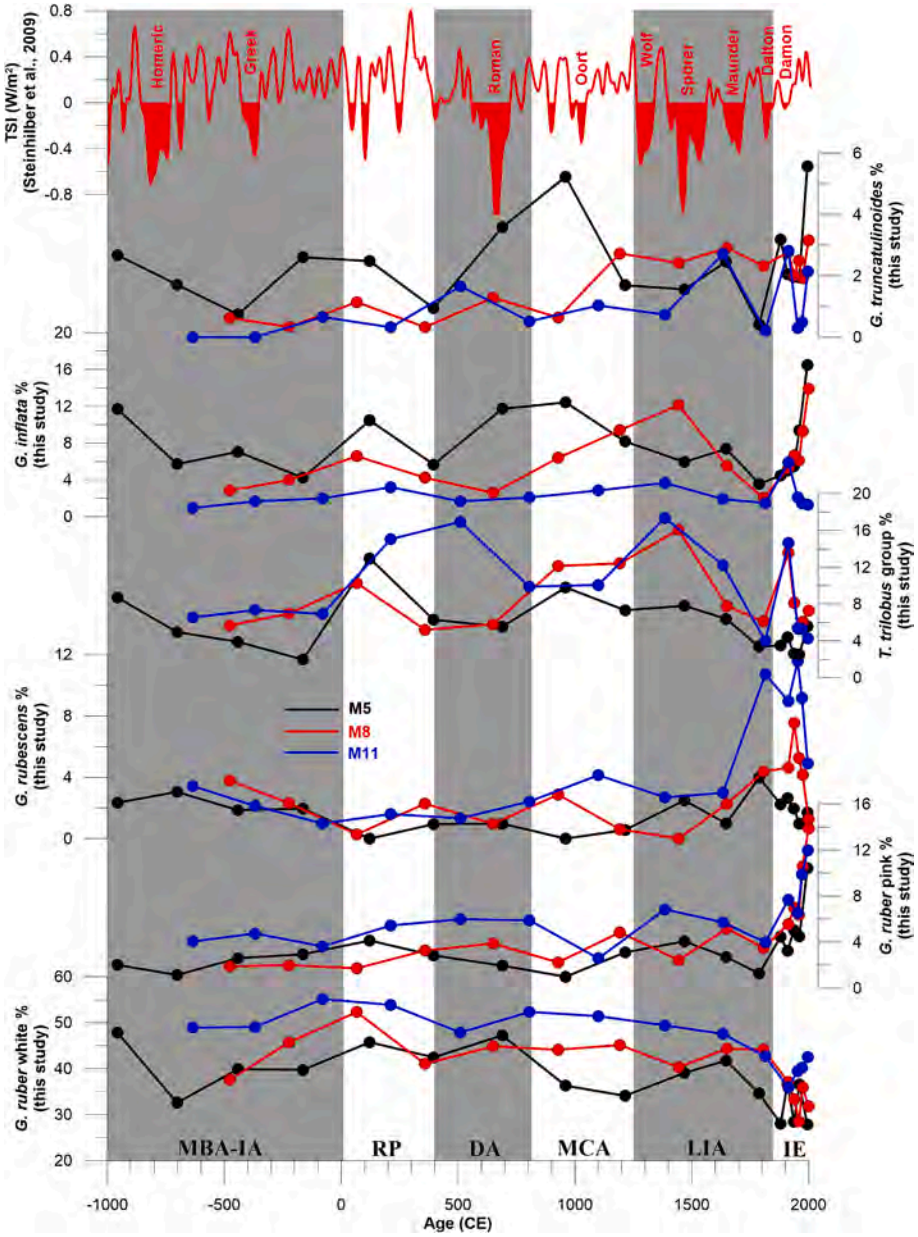

Fig. 4. Downcore variations of selected planktonic foraminiferal species (%) in cores M5 (black lines), M8 (red lines) and M11 (blue lines), plotted *versus* age expressed in years CE. The total solar irradiation (W/m^2) by Steinhilber et al. (2009) is also shown. Grey and white boxes show preindustrial changes in climate and society, drawn following Abram et al. (2016), Büntgen et al. (2016) and Margaritelli et al. (2016). MBA-IA: Middle Bronze Age-Iron Age; RP: Roman Period; Dark Age; MCA: Medieval Climate Anomaly; LIA: Little Ice Age; IE: Industrial Era. (For interpretation of the references to colour in this figure legend, the reader is referred to the web version of this article.)

three different cores, likely because of different hydrological settings, for instance in terms of MAW and LIW pathways (Fig. 1). In any case, our study struggles to identify distinctive water column dynamics (*e.g.* stratification and surface productivity phases) linked to Total Solar Irradiation variability, and even to distinguish peculiar assemblages linked to different historical climatic periods, as reported in previous high-resolution studies (Cisneros et al., 2016; Incarbona et al., 2023; Incarbona et al., 2019; Incarbona et al., 2010; Margaritelli et al., 2018). Most of the species dwelling in cold surface and productive water, like *G. glutinata*, *G. bulloides*, *T. quinqueloba* and *N. incompta,* shows abundance peaks close to Middle Bronze Age (MBA)-IE, Dark Ages (DA) and the beginning and end of LIA (Figs. 4-6). However, the low-resolution of species abundance signals and the frequent signal offset hamper further in-depth reasoning. Even the number of individuals per gram of sediment and the Shannon-Wiener diversity curve do show a variability since the IE which is higher than the rest of the record (Fig. 6).

Planktonic foraminiferal raw data are available in SM3, Table S3.

8.2. Multispecies stable isotopes

Globigerinoides ruber $\delta^{18}O$ values vary between about 0.9 and 0.1 ‰ and exhibit significant (> 0.4 ‰) fluctuations, for instance in M11 since 1900 CE (Fig. 7). *Uvigerina peregrina* $\delta^{18}O$ values are rather contained in magnitude, varying between about 2.2 and 1.9 ‰ (Fig. 7).

Globigerinoides ruber $\delta^{13}C$ values vary between about 1.5 and 0.9 ‰ and show a distinct trend to heavier values in core M11 (Fig. 7). *Uvigerina peregrina* $\delta^{13}C$ values in the southernmost M11 core are distinctly lighter than in M5 and M8, showing an oscillating pattern between 0.6 and -0.4 ‰ until 1900 CE, thereafter the isotopic analysis was not carried out because of an inadequate number (absence) of benthic

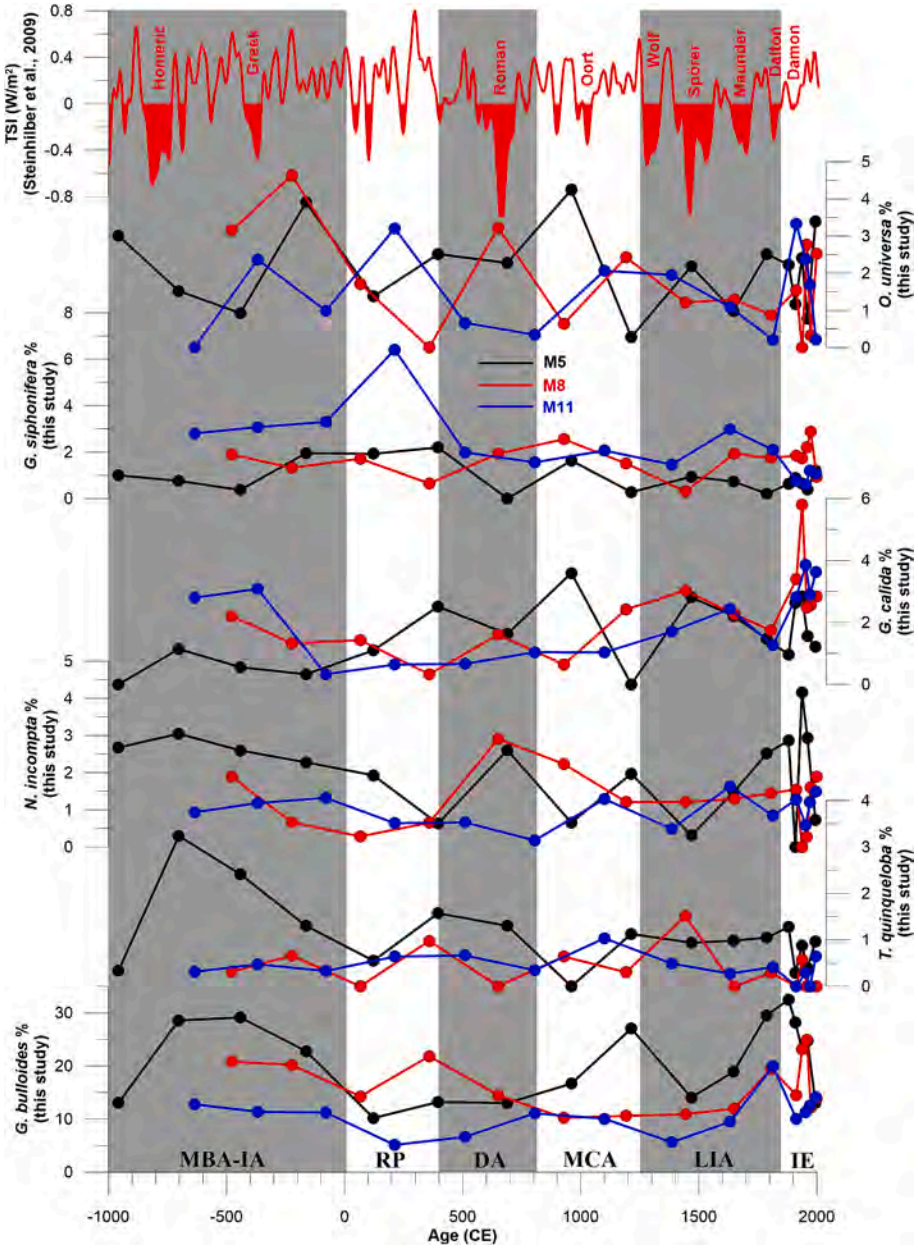

Fig. 5. Downcore variations of selected planktonic foraminiferal species (%) in cores M5 (black lines), M8 (red lines) and M11 (blue lines), plotted *versus* age expressed in years CE. The total solar irradiation (W/m^2) by Steinhilber et al. (2009) is also shown. Grey and white boxes show preindustrial changes in climate and society, drawn following Abram et al. (2016), Büntgen et al. (2016) and Margaritelli et al. (2016). MBA-IA: Middle Bronze Age-Iron Age; RP: Roman Period; Dark Age; MCA: Medieval Climate Anomaly; LIA: Little Ice Age; IE: Industrial Era. (For interpretation of the references to colour in this figure legend, the reader is referred to the web version of this article.)

specimens (Fig. 7). Distinctly lighter δ^{13}C *U. peregrina* values in M11 are likely due to enhanced primary productivity in the northern Libyan coast, as observed in satellite-derived estimates by D'Ortenzio and Ribera d'Alcalà (2009) and Salgado-Hernanz et al. (2022).

In general, both planktonic and benthic δ^{18}O values are rather misaligned among the different three cores: oxygen isotopic signals seem to be more similar for M11 and M8 cores, especially in *G. ruber* shell analysis (Fig. 7). Lacking global (sea-level variations/ice volume accumulation) and hemispheric (SST variations for Dansgaard-Oeschger events) factors, the low-magnitude variability imprinted in the oxygen isotopic signal is likely due to changes in surface and bottom water paths and/or mesoscale features activity that differently impacted M5, M8 and M11 sites (Fig. 1). For instance, M5 core location is adjacent to the semipermanent meso-scale Medina cyclonic gyre and M11 core location is in the southern vein pathway of LIW. As for planktonic foraminifera assemblages, low-resolution and the frequent signal offset restrict our discussion on stable isotope results to the IE.

8.3. Response to global warming

Focussing on the last two centuries, test accumulation rates are again modified since the IE, increasing more than three times at the beginning of the twentieth century and declining after the 1940-1960 CE (Fig. 8A). This behaviour is almost the same as those recently reported from the Alboran and Balearic Seas (Fig. 8B), which importantly claims that the planktonic foraminifera productivity decreased under the anthropogenic pressure due to the global warming (Pallacks et al., 2021). Our results in the Sicily Channel supports this conclusion, widening the

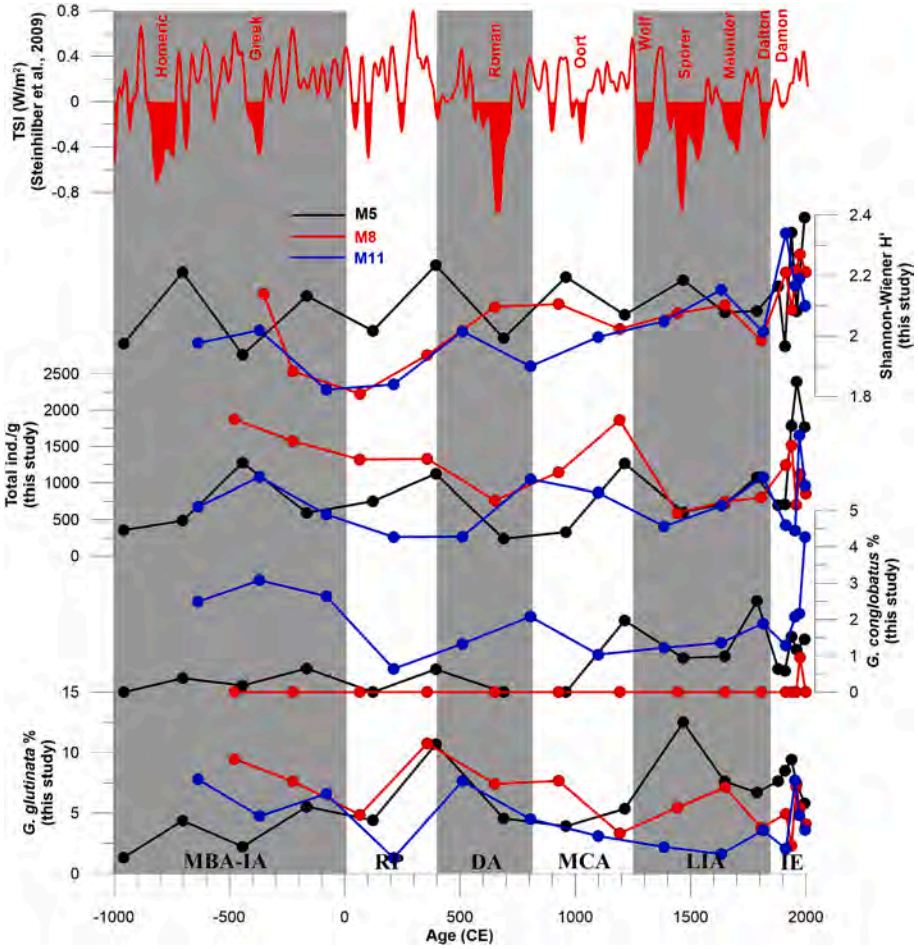

Fig. 6. Downcore variations of selected planktonic foraminiferal species (%), number of individuals per gram of sediment and Shannon-Wiener diversity curve in cores M5 (black lines), M8 (red lines) and M11 (blue lines), plotted *versus* age expressed in years CE. The total solar irradiation (W/m^2) by Steinhilber et al. (2009) is also shown. Grey and white boxes show preindustrial changes in climate and society, drawn following Abram et al. (2016), Büntgen et al. (2016) and Margaritelli et al. (2016). MBA-IA: Middle Bronze Age-Iron Age; RP: Roman Period; Dark Age; MCA: Medieval Climate Anomaly; LIA: Little Ice Age; IE: Industrial Era. (For interpretation of the references to colour in this figure legend, the reader is referred to the web version of this article.)

spatial area of this phenomenon to a large (western-central) portion of the Mediterranean Sea. Further, we observe that the ongoing decline in planktonic foraminiferal accumulation rate since the second half of the twentieth century is associated with the most abrupt temperature rise in regional and global records (Figs. 8C-D). Interestingly, this event has been preceded by increasing test accumulation rates in both the western and central Mediterranean Sea, between ~1920 and 1960 CE (Figs. 8A-B), when the positive AMO phase was occurring (Fig. 8E). As the AMO Index variability drives different large-scale atmospheric circulation patterns and SST values over the Mediterranean (Marullo et al., 2011; Zampieri et al., 2017), we can speculate that its positive mode may have fostered winter/spring surface productivity in the Sicily Channel as proposed by Incarbona et al. (2019). In Fig. 8E it is also evident that a new positive AMO phase is established since ~2000 CE, without a clear response in increasing planktonic foraminiferal accumulation rates. Two explanations may be raised for such a behaviour: i) the M5, M8 and M11 do not record signals on transition to 2000 CE, because missing samples at the top of the record; ii) AMO positive mode is not still effective under very high regional and global temperatures. The latter explanation would be supported by the very low number of planktonic foraminiferal individuals found during spring 2013 CE throughout the Mediterranean Sea (Mallo et al., 2017), and would be compatible with Mediterranean planktonic foraminiferal data from global compilations (Chaabane et al., 2023; de Garidel-Thoron et al., 2022) and with observed low productivity in the area during the'50-'70 surveys (Cifelli, 1974).

Importantly, the planktonic foraminifera productivity increase/decrease in the IE matches with a lower/higher number of Large Azores High events in winter (Cresswell-Clay et al., 2022) and strengthened/weakened paleostorm activity in the Gulf of Lions (Sabatier et al., 2012) (Figs. 8F-G).

The exceptional area extent and frequency of the Azores High in winter since the IE, has brought anomalous dry conditions over western Europe and western-central Mediterranean region and seems to be a direct effect of Global Warming and CO_2 level exponential increase (Fig. 8H) (Cresswell-Clay et al., 2022).

Planktonic foraminiferal data, especially for the northernmost cores M5-M8, clearly show that increased Large Azores High Events during the IE would have modified the surface marine environment (Fig. 9). The persistent atmospheric high-pressure ridge over the western-central Mediterranean Sea would have reduced winter productivity, by inhibiting vertical mixing in the water column and surface water nutrient fuelling, as further supported by the significant decrease in the Gulf of Lions paleostorm activity (Fig. 8G) (Sabatier et al., 2012). Surface productivity and DCM species declined in the IE with a short increase in the M8 core ~1960 CE, while the Azores High was relaxing (Fig. 9B-C). Winter mixed layer taxa shows an opposite pattern, pointing out that the Large Azores High Events significantly limit the winter vertical mixing extent down to only a few hundred metres (Fig. 9D). This change in the planktonic foraminiferal productivity is evidenced by the *G. bulloides* / *G. bulloides* + *G. inflata* + *G. truncatulinoides* ratio, already used in the

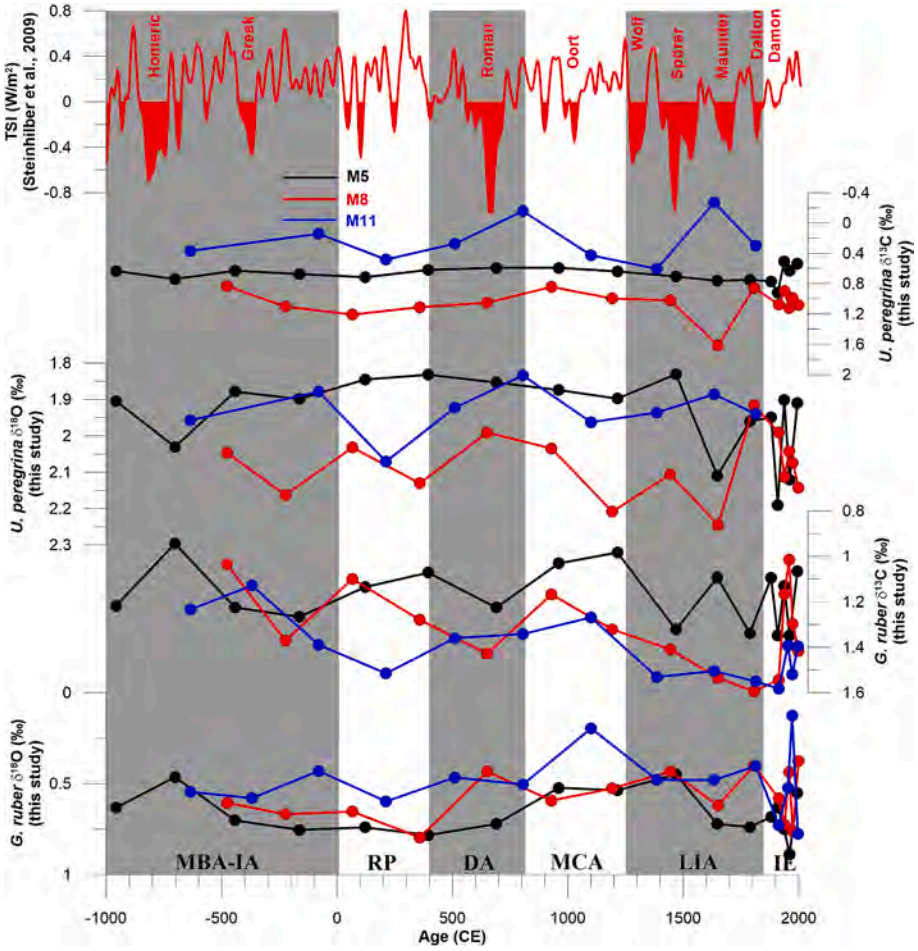

Fig. 7. Downcore variations of *G. ruber* and *U. peregrina* $\delta^{18}O$ and $\delta^{13}C$ in cores M5 (black lines), M8 (red lines) and M11 (blue lines), plotted *versus* age expressed in years CE. The total solar irradiation (W/m^2) by Steinhilber et al. (2009) is also shown. Grey and white boxes show preindustrial changes in climate and society, drawn following Abram et al. (2016), Büntgen et al. (2016) and Margaritelli et al. (2016). MBA-IA: Middle Bronze Age-Iron Age; RP: Roman Period; Dark Age; MCA: Medieval Climate Anomaly; LIA: Little Ice Age; IE: Industrial Era. (For interpretation of the references to colour in this figure legend, the reader is referred to the web version of this article.)

Sicily Channel (Incarbona et al., 2019), that shows a steeper gradient in the second half of the 20th century, in response to the highest number of Large Azores High Events (Fig. 9E).

Tropical and subtropical taxa do not show significant variability, except for the short decrease ~1960 CE, in coincidence of the planktonic foraminiferal accumulation rate increase (Fig. 9F). Oxygen isotope data would support lacking significant modification in the summer marine environment. The $\Delta\delta^{18}O$ between *U. peregrina* and *G. ruber*, that highlights the stratification strength in summer (Incarbona et al., 2013; Incarbona and Sprovieri, 2020), do not show significant changes in amplitude over the last two centuries (Fig. 9G).

The ecological inferences above discussed point to the radical transformation of the Sicily Channel environment. It is being impoverished and transformed into prevalent summer productivity (Fig. 2), like eastern settings. Eastern Mediterranean oligotrophy has been widening its influence into the eastern flank of the Sicily Channel. This area has been relatively productive over, at least, the last two glacial/interglacial cycles, as witnessed by planktonic foraminiferal assemblages (Incarbona et al., 2013; Sprovieri et al., 2006; Sprovieri et al., 2003). Our results further support reports of the Mediterranean Sea tropicalization and invasion of alien species, happening through a progressive westward direction (Katsanevakis et al., 2014; Peleg et al., 2020). We set the timing of this phenomenon, at the onset of the IE and with a recrudescence since the second half of the 19th century and suggest that the persistent atmospheric high-pressure ridge over the western-central Mediterranean Sea may have played a major role.

9. Conclusion

We have analyzed planktonic foraminiferal content from three short sediment cores (M5, M8 and M11) recovered in a North/South transect in the eastern Sicily Channel. The decadal-scale resolution across the IE led us to verify the response of assemblages to the ongoing climate change.

Signals of modifications across the preindustrial/industrial Era are documented by different species, especially since 1900-1950 CE, like abundance decrease in *G. bulloides* and abundance increase in *G. inflata* and *G. truncatulinoides*. This means that the most significant modern features in Sicily Channel planktonic foraminifera assemblages, such as high abundances of *G. ruber* pink rather than *G. ruber* white or *G. inflata* rather than *G. bulloides* (Pujol and Vergnaud Grazzini, 1995), have been occurring since the beginning of the IE.

The planktonic foraminiferal productivity decreased over the IE, with a significant acceleration after the second half of the 20th century. This observation is consistent with previous studies performed the Alboran and Balearic Seas (Pallacks et al., 2021). Probably, the productivity decline is linked to the establishment of an exceptional and persistent atmospheric high-pressure ridge over the western-central Mediterranean Sea, by a higher number of winter Large Azores High Events, which is in turn due to the ongoing global warming (Cresswell-

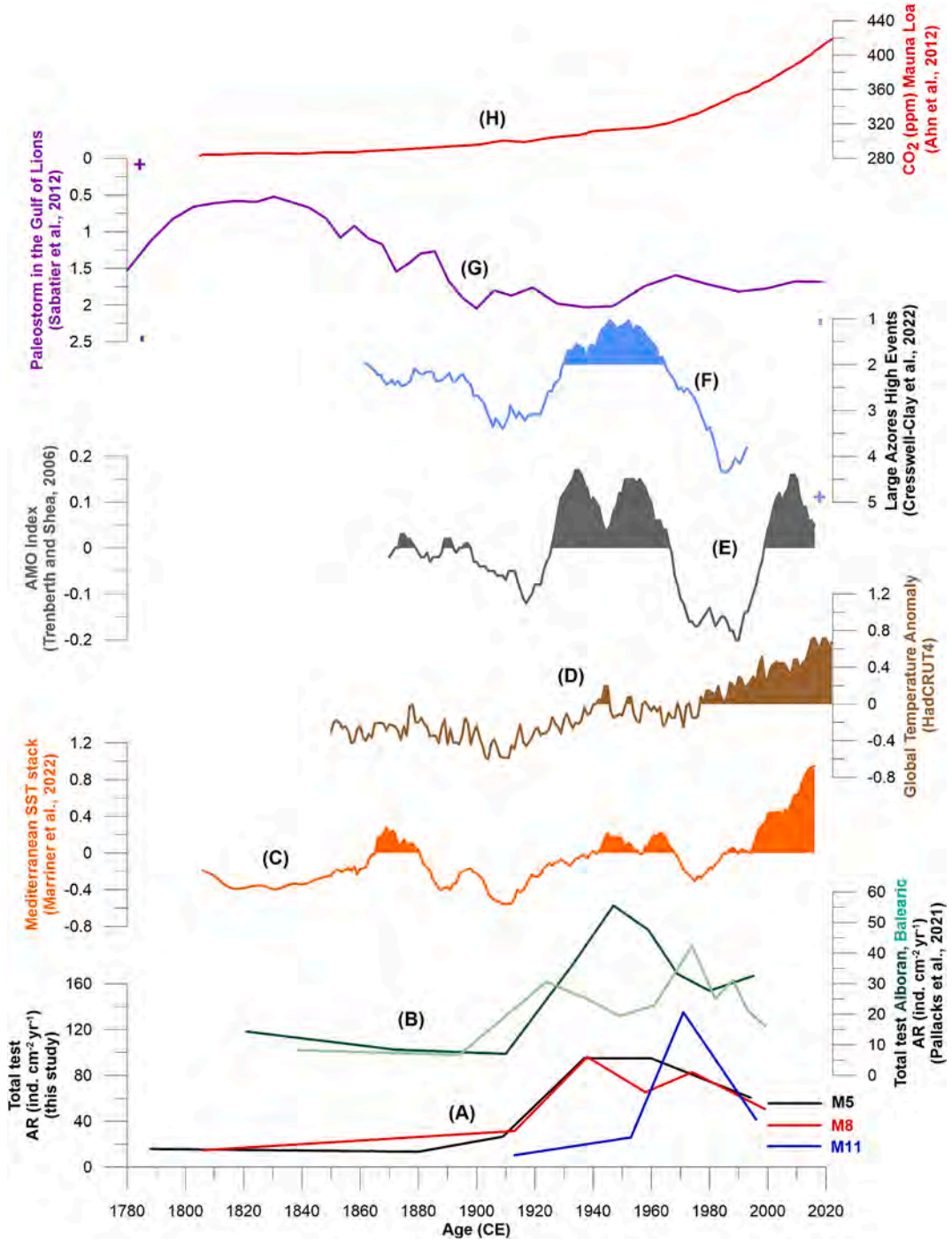

Fig. 8. (A) Downcore variations of planktonic foraminiferal total test accumulation rates (individuals on squared cm per year), in cores M5 (black lines), M8 (red lines) and M11 (blue lines). (B) Downcore variations of planktonic foraminifera total test accumulation rates (individuals on squared cm per year), in Alboran and Balearic Seas (green and light green lines) (Pallacks et al., 2021). (C) Mediterranean SST (°C) stack (orange line) (Marriner et al., 2022). (D) Global temperature anomaly SST (°C) (brown line) (HadCRUT4). (E) Atlantic Multidecadal Oscillation (AMO) Index (grey line) (Trenberth and Shea, 2006). (F) Large Azores High Events (light blue line) (Cresswell-Clay et al., 2022). (G) Reconstructed paleostorm activity in the Gulf of Lions (purple line) (Sabatier et al., 2012). (H) CO_2 levels in ppm (red line) from the Mauna Loa instrumental record and Antarctica ice cores (Ahn et al., 2012). All curves are plotted *versus* age expressed in years CE. (For interpretation of the references to colour in this figure legend, the reader is referred to the web version of this article.)

Clay et al., 2022). Surface productivity and DCM species declines since the IE, with a steeper gradient in the second half of the 20th century, opposed to a simultaneous increase of winter mixed layer taxa. This shift points out that Azores High exceptional winter activity significantly limited the water column vertical mixing and the photic zone nutrient fuelling.

This study claims that the Sicily Channel area is an environment subject to a radical transformation. It is being transformed into prevalent summer productivity, like the eastern oligotrophic part of the Mediterranean Sea. Our findings indicate that the Mediterranean area in the near future is undergoing a process of oligotrophy. However, additional studies covering other basins are needed to support our findings and to better constrain the ongoing change.

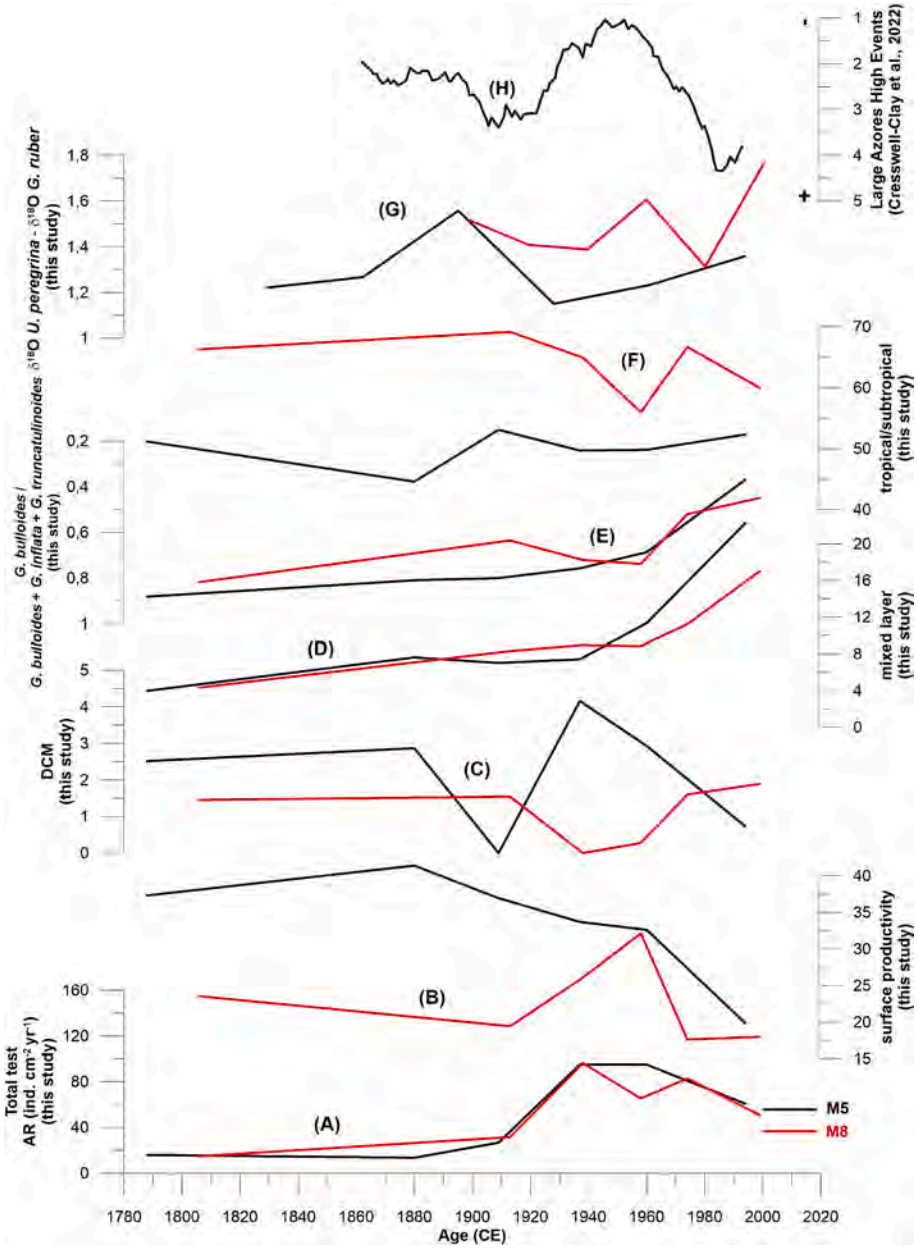

Fig. 9. (A) Downcore variations of planktonic foraminiferal total test accumulation rates (individuals on squared cm per year), in cores M5 (black lines) and M8 (red lines). (B) (A) Downcore variations of planktonic foraminiferal surface productivity species (%), in cores M5 (black lines) and M8 (red lines). (C) Downcore variations of planktonic foraminiferal DCM species (*N. incompta*) (%), in cores M5 (black lines) and M8 (red lines). (D) Downcore variations of planktonic foraminiferal winter mixed layer species (%), in cores M5 (black lines) and M8 (red lines). (E) Downcore variations of planktonic foraminiferal ratio between *G. bulloides versus G. inflata* and *G. truncatulinoides* (Incarbona et al., 2019), in cores M5 (black lines) and M8 (red lines). (F) Downcore variations of planktonic foraminiferal tropical/subtropical species (%), in cores M5 (black lines) and M8 (red lines). (G) Downcore variations of *U. peregrina – G. ruber* $\delta^{18}O$, in cores M5 (black lines) and M8 (red lines). (H) Large Azores High Events (black line) (Cresswell-Clay et al., 2022). All curves are plotted *versus* age expressed in years CE. (For interpretation of the references to colour in this figure legend, the reader is referred to the web version of this article.)

CRediT authorship contribution statement

Ferraro Serena: Writing – review & editing, Investigation, Formal analysis, Conceptualization. **Alessandro Incarbona:** Writing – original draft, Data curation, Conceptualization. **Sergio Bonomo:** Writing – review & editing, Conceptualization. **Lucilla Capotondi:** Writing – review & editing, Conceptualization. **Luigi Giaramita:** Writing – review & editing. **Leonardo Langone:** Writing – review & editing, Investigation, Data curation, Conceptualization. **Nereo Preto:** Writing – review & editing, Formal analysis, Data curation, Conceptualization. **Giovanni Surdi:** Writing – review & editing. **Elena Zanola:** Writing – review & editing, Conceptualization. **Giorgio Tranchida:** Writing – review & editing, Supervision.

Declaration of competing interest

The authors declare that they have no known competing financial interests or personal relationships that could have appeared to influence the work reported in this paper.

Data availability

Data will be available on Pangaea. They are already attached in Supplementary Material.

Ackowledgments

We are grateful to two anonymous reviewers and to Fabienne Marret-Davies for helpful comments and suggestions. AI acknowledges the support received from the NBFC, funded by the Italian Ministry of University and Research, PNRR, Missione 4 Componente 2, project CN00000033. GT acknowledges the support received from the SALT Project. We thank Angelo Bonanno and the ECORIM group of CNR-IAS who recovered sedimentary cores during the MedSudMed cruise.

Appendix A. Supplementary data

Supplementary data to this article can be found online at https://doi.org/10.1016/j.gloplacha.2024.104532.

References

Abram, N.J., McGregor, H.V., Tierney, J.E., Evans, M.N., McKay, N.P., Kaufman, D.S., Thirumalai, K., Martrat, B., Goosse, H., Phipps, S.J., Steig, E.J., Kilbourne, K.H., Saenger, C.P., Zinke, J., Leduc, G., Addison, J.A., Mortyn, P.G., Seidenkrantz, M.S., Sicre, M.A., Selvaraj, K., Filipsson, H.L., Neukom, R., Gergis, J., Curran, M.A.J., Von Gunten, L., 2016. Early onset of industrial-era warming across the oceans and continents. Nature 536, 411–418. https://doi.org/10.1038/nature19082.

Ahn, J., Brook, E.J., Mitchell, L., Rosen, J., McConnell, J.R., Taylor, K., Etheridge, D., Rubino, M., 2012. Atmospheric CO2 over the last 1000 years: a high-resolution record from the West Antarctic Ice Sheet (WAIS) divide ice core. Global Biogeochem. Cycles 26. https://doi.org/10.1029/2011GB004247.

Allen, J.I., Somerfield, P.J., Siddorn, J., 2002. Primary and bacterial production in the Mediterranean Sea: a modelling study. J. Mar. Syst. 33–34, 473–495. https://doi.org/10.1016/S0924-7963(02)00072-6.

Azibeiro, L.A., Kučera, M., Jonkers, L., Cloke-Hayes, A., Sierro, F.J., 2023. Nutrients and hydrography explain the composition of recent Mediterranean planktonic foraminiferal assemblages. Mar Micropaleontol 179, 102201. https://doi.org/10.1016/j.marmicro.2022.102201.

Béranger, K., Mortier, L., Gasparini, G.P., Gervasio, L., Astraldi, M., Crépon, M., 2004. The dynamics of the Sicily Strait: a comprehensive study from observations and models. Deep Sea Res 2 Top Stud Oceanogr 51, 411–440. https://doi.org/10.1016/j.dsr2.2003.08.004.

Béthoux, J.P., 1979. Budgets of the Mediterranean Sea. Their dependence on the local climate and on the characteristics of the Atlantic waters. Oceanol. Acta 2, 157–163.

Bethoux, J.P., Gentili, B., Morin, P., Nicolas, E., Pierre, C., Ruiz-Pino, D., 1999. The Mediterranean Sea: a miniature ocean for climatic and environmental studies and a key for the climatic functioning of the North Atlantic. Prog. Oceanogr. 44, 131–146. https://doi.org/10.1016/S0079-6611(99)00023-3.

Bijma, J., Faber, W., Hemleben, C., 1990. Temperature and salinity limits for growth and survival of some planktonic foraminifers in laboratory cultures. The Journal of Foraminiferal Research 20, 95–116.

Blaauw, M., Christen, J.A., 2011. Flexible paleoclimate age-depth models using an autoregressive gamma process. Bayesian Anal. 6, 457–474. https://doi.org/10.1214/11-BA618.

Büntgen, U., Myglan, V.S., Ljungqvist, F.C., McCormick, M., Di Cosmo, N., Sigl, M., Jungclaus, J., Wagner, S., Krusic, P.J., Esper, J., Kaplan, J.O., de Vaan, M.A.C., Luterbacher, J., Wacker, L., Tegel, W., Kirdyanov, A.V., 2016. Cooling and societal change during the late Antique Little Ice Age from 536 to around 660 AD. Nat. Geosci. 9, 231–236. https://doi.org/10.1038/ngeo2652.

Chaabane, S., de Garidel-Thoron, T., Giraud, X., Schiebel, R., Beaugrand, G., Brummer, G.-J., Casajus, N., Greco, M., Grigoratou, M., Howa, H., Jonkers, L., Kucera, M., Kuroyanagi, A., Meilland, J., Monteiro, F., Mortyn, G., Almogi-Labin, A., Asahi, H., Avnaim-Katav, S., Bassinot, F., Davis, C.V., Field, D.B., Hernández-Almeida, I., Herut, B., Hosie, G., Howard, W., Jentzen, A., Johns, D.G., Keigwin, L., Kitchener, J., Kohfeld, K.E., Lessa, D.V.O., Manno, C., Marchant, M., Ofstad, S., Ortiz, J.D., Post, A., Rigual-Hernandez, A., Rillo, M.C., Robinson, K., Sagawa, T., Sierro, F., Takahashi, K.T., Torfstein, A., Venancio, I., Yamasaki, M., Ziveri, P., 2023. The FORCIS database: a global census of planktonic Foraminifera from ocean waters. Sci Data 10, 354. https://doi.org/10.1038/s41597-023-02264-2.

Checa, H., Margaritelli, G., Pena, L.D., Frigola, J., Cacho, I., Rettori, R., Lirer, F., 2020. High resolution paleo-environmental changes during the Sapropel 1 in the North Ionian Sea, Central Mediterranean. Holocene 30, 1504–1515. https://doi.org/10.1177/0959683620941095.

Cifelli, R., 1974. Planktonic foraminifera from the Mediterranean and adjacent Atlantic waters (Cruise 49 of the ATLANTIS II, 1969). J. Foraminifer. Res. 4, 171–183. https://doi.org/10.2113/gsjfr.4.4.171.

Cisneros, M., Cacho, I., Frigola, J., Canals, M., Masqué, P., Martrat, B., Casado, M., Grimalt, J.O., Pena, L.D., Margaritelli, G., Lirer, F., 2016. Sea surface temperature variability in the Central-Western Mediterranean Sea during the last 2700 years: a multi-proxy and multi-record approach. Climate of the Past 12, 849–869. https://doi.org/10.5194/cp-12-849-2016.

Comas-Bru, L., McDermott, F., 2014. Impacts of the EA and SCA patterns on the European twentieth century NAO–winter climate relationship. Q. J. Roy. Meteorol. Soc. 140, 354–363. https://doi.org/10.1002/qj.2158.

Cresswell-Clay, N., Ummenhofer, C.C., Thatcher, D.L., Wanamaker, A.D., Denniston, R. F., Asmerom, Y., Polyak, V.J., 2022. Twentieth-century Azores High expansion unprecedented in the past 1,200 years. Nat. Geosci. 15, 548–553. https://doi.org/10.1038/s41561-022-00971-w.

de Garidel-Thoron, T., Chaabane, S., Giraud, X., Meilland, J., Jonkers, L., Kucera, M., Brummer, G.-J.A., Grigoratou, M., Monteiro, F.M., Greco, M., Mortyn, P.G., Kuroyanagi, A., Howa, H., Beaugrand, G., Schiebel, R., 2022. The Foraminiferal Response to climate Stressors Project: Tracking the Community Response of Planktonic Foraminifera to Historical climate Change. Front. Mar. Sci. 9 https://doi.org/10.3389/fmars.2022.827962.

D'Ortenzio, F., Ribera d'Alcalà, M., 2009. On the trophic regimes of the Mediterranean Sea: a satellite analysis. Biogeosciences 6, 139–148. https://doi.org/10.5194/bg-6-139-2009.

Enfield, D.B., Mestas-Nunez, A.M., Trimble, P.J., 2001. The Atlantic multidecadal oscillation and its relation to rainfall and river flows in the continental U.S. Geophys. Res. Lett. 28, 2077–2080.

Fairbanks, R.G., Wiebe, P.H., 1980. Foraminifera and Chlorophyll Maximum: Vertical distribution, Seasonal Succession, and Paleoceanographic significance. Science 209, 1524–1526.

Frignani, M., Langone, L., 1991. Accumulation rates and137Cs distribution in sediments off the Po River delta and the Emilia-Romagna coast (northwestern Adriatic Sea, Italy). Cont. Shelf Res. 11, 525–542. https://doi.org/10.1016/0278-4343(91)90009-U.

Gasparini, G.P., Ortona, A., Budillon, G., Astraldi, M., Sansone, E., 2005. The effect of the Eastern Mediterranean Transient on the hydrographic characteristics in the Strait of Sicily and in the Tyrrhenian Sea. Deep Sea Res 1 Oceanogr Res Pap 52, 915–935. https://doi.org/10.1016/j.dsr.2005.01.001.

Giamali, C., Kontakiotis, G., Koskeridou, E., Ioakim, C., Antonarakou, A., 2020. Key Environmental Factors Controlling Planktonic Foraminiferal and Pteropod Community's Response to late Quaternary Hydroclimate changes in the South Aegean Sea (Eastern Mediterranean). J Mar Sci Eng 8. https://doi.org/10.3390/jmse8090709.

Giamali, C., Kontakiotis, G., Antonarakou, A., Koskeridou, E., 2021. Ecological constraints of plankton bio-indicators for water column stratification and productivity: a case study of the holocene north aegean sedimentary record. J Mar Sci Eng 9. https://doi.org/10.3390/jmse9111249.

Giorgi, F., Lionello, P., 2008. Climate change projections for the Mediterranean region. Glob Planet Change 63, 90–104. https://doi.org/10.1016/j.gloplacha.2007.09.005.

Hemleben, C., Spindler, M., Anderson, O.R., 1989. Modern Planktonic Foraminifera. Springer-Verlag, Berlin, Heidelberg. https://doi.org/10.1007/978-1-4612-3544-6.

Incarbona, A., Sprovieri, M., 2020. The Postglacial Isotopic Record of Intermediate Water Connects Mediterranean Sapropels and Organic-Rich Layers. Paleoceanogr Paleoclimatol 35. https://doi.org/10.1029/2020PA004009 e2020PA004009.

Incarbona, A., Ziveri, P., Di Stefano, E., Lirer, F., Mortyn, G., Patti, B., Pelosi, N., Sprovieri, M., Tranchida, G., Vallefuoco, M., Albertazzi, S., Bellucci, L.G., Bonanno, A., Bonomo, S., Censi, P., Ferraro, L., Giuliani, S., Mazzola, S., Sprovieri, R., 2010. The Impact of the Little Ice Age on Coccolithophores in the Central Mediterranea Sea. Clim. Past 6, 795–805. https://doi.org/10.5194/cp-6-795-2010.

Incarbona, A., Sprovieri, M., Di Stefano, A., Di Stefano, E., Salvagio Manta, D., Pelosi, N., Ribera d'Alcalà, M., Sprovieri, R., Ziveri, P., Di, A., Di, E., Salvagio, D., Pelosi, N., Ribera, M., Sprovieri, R., Ziveri, P., 2013. Productivity modes in the mediterranean sea during dansgaard-oeschger (20,000-70,000yr ago) oscillations. Palaeogeogr Palaeoclimatol Palaeoecol 392, 128–137. https://doi.org/10.1016/j.palaeo.2013.09.023.

Incarbona, A., Martrat, B., Mortyn, P.G., Sprovieri, M., Ziveri, P., Gogou, A., Jordà, G., Xoplaki, E., Luterbacher, J., Langone, L., Marino, G., Rodríguez-Sanz, L., Triantaphyllou, M., Di Stefano, E., Grimalt, J.O., Tranchida, G., Sprovieri, R., Mazzola, S., 2016. Mediterranean circulation perturbations over the last five centuries: Relevance to past Eastern Mediterranean Transient-type events. Sci. Rep. 6 https://doi.org/10.1038/srep29623.

Incarbona, A., Jonkers, L., Ferraro, S., Sprovieri, R., Tranchida, G., 2019. Sea Surface Temperatures and Paleoenvironmental Variability in the Central Mediterranean during Historical Times Reconstructed using Planktonic Foraminifera. Paleoceanogr Paleoclimatol 34, 394–408. https://doi.org/10.1029/2018PA003529.

Incarbona, A., Bonomo, S., Cacho, I., Lirer, F., Margaritelli, G., Pecoraro, D., Ziveri, P., 2023. Solar forcing for nutricline depth variability inferred by coccoliths in the pre-industrial northwestern Mediterranean. Glob Planet Change 224, 104102. https://doi.org/10.1016/j.gloplacha.2023.104102.

Jonkers, L., Kučera, M., 2015. Global analysis of seasonality in the shell flux of extant planktonic Foraminifera. Biogeosciences 12, 2207–2226. https://doi.org/10.5194/bg-12-2207-2015.

Jonkers, L., Hillebrand, H., Kucera, M., 2019. Global change drives modern plankton communities away from the pre-industrial state. Nature 570, 372–375. https://doi.org/10.1038/s41586-019-1230-3.

Josey, S.A., Somot, S., Tsimplis, M., 2011. Impacts of atmospheric modes of variability on Mediterranean Sea surface heat exchange. J Geophys Res Oceans 116, 1–15. https://doi.org/10.1029/2010JC006685.

Jouini, M., Béranger, K., Arsouze, T., Beuvier, J., Thiria, S., Crépon, M., Taupier-Letage, I., 2016. The Sicily Channel surface circulation revisited using a neural clustering analysis of a high-resolution simulation. J Geophys Res Oceans 121, 4545–4567. https://doi.org/10.1002/2015JC011472.

Katsanevakis, S., Coll, M., Piroddi, C., Steenbeek, J., Ben Rais Lasram, F., Zenetos, A., Cardoso, A.C., 2014. Invading the Mediterranean Sea: biodiversity patterns shaped by human activities. Front. Mar. Sci. 1 https://doi.org/10.3389/fmars.2014.00032.

Klein, P., Coste, B., 1984. Effects of wind-stress variability on nutrient transport into the mixed layer. Deep Sea Research Part a. Oceanographic Research Papers 31, 21–37. https://doi.org/10.1016/0198-0149(84)90070-0.

Kontakiotis, G., Efstathiou, E., Zarkogiannis, S.D., Besiou, E., Antonarakou, A., 2021. Latitudinal Differentiation among Modern Planktonic Foraminiferal Populations of Central Mediterranean: Species–Specific Distribution Patterns and Size Variability. J Mar Sci Eng 9. https://doi.org/10.3390/jmse9050551.

Krom, M.D., Emeis, K.C., Van Cappellen, P., 2010. Why is the Eastern Mediterranean phosphorus limited? Prog. Oceanogr. 85, 236–244. https://doi.org/10.1016/j.pocean.2010.03.003.

Lermusiaux, P.F.J., Robinson, A.R., 2001. Features of dominant mesoscale variability, circulation patterns and dynamics in the strait of sicily. Deep Sea Res 1 Oceanogr Res Pap 48, 1953–1997. https://doi.org/10.1016/S0967-0637(00)00114-X.

Lionello, P., 2012. The Climate of the Mediterranean Region: From the Past to the Future, 1st ed. Elsevier Inc. https://doi.org/10.1016/B978-0-12-416042-2.00009-4

Lirer, F., Sprovieri, M., Ferraro, L., Vallefuoco, M., Capotondi, L., Cascella, A., Petrosino, P., Insinga, D.D., Pelosi, N., Tamburrino, S., Lubritto, C., 2013. Integrated stratigraphy for the Late Quaternary in the eastern Tyrrhenian Sea. Quaternary International 292, 71–85. https://doi.org/10.1016/j.quaint.2012.08.2055. ISSN 1040-6182.

Malanotte-Rizzoli, P., Hecht, A., 1988. Large-scale properties of the eastern Mediterranean: a review. Oceanol. Acta 11, 323–335. https://doi.org/10.1016/S0967-0645(99)00020-X.

Mallo, M., Ziveri, P., Mortyn, P.G., Schiebel, R., Grelaud, M., 2017. Low planktic foraminiferal diversity and abundance observed in a spring 2013 west–east Mediterranean Sea plankton tow transect. Biogeosciences 14, 2245–2266. https://doi.org/10.5194/bg-14-2245-2017.

Margaritelli, G., Vallefuoco, M., Di Rita, F., Capotondi, L., Bellucci, L.G., Insinga, D.D., Petrosino, P., Bonomo, S., Cacho, I., Cascella, A., Ferraro, L., Florindo, F., Lubritto, C., Lurcock, P.C., Magri, D., Pelosi, N., Rettori, R., Lirer, F., 2016. Marine response to climate changes during the last five millennia in the Central Mediterranean Sea. Glob Planet Change 142, 53–72. https://doi.org/10.1016/j.gloplacha.2016.04.007.

Margaritelli, G., Cisneros, M., Cacho, I., Capotondi, L., Vallefuoco, M., Rettori, R., Lirer, F., 2018. Climatic variability over the last 3000 years in the central - western Mediterranean Sea (Menorca Basin) detected by planktonic foraminifera and stable isotope records. Glob Planet Change 169, 179–187. https://doi.org/10.1016/j.gloplacha.2018.07.012.

Margaritelli, G., Lirer, F., Schroeder, K., Alberico, I., Dentici, M.P., Caruso, A., 2020. Globorotalia truncatulinoides in Central - Western Mediterranean Sea during the Little Ice Age. Mar Micropaleontol 161, 101921. https://doi.org/10.1016/j.marmicro.2020.101921.

Margaritelli, G., Lirer, F., Schroeder, K., Cloke-Hayes, A., Caruso, A., Capotondi, L., Broggy, T., Cacho, I., Sierro, F.J., 2022. Globorotalia truncatulinoides in the Mediterranean Basin during the Middle–late Holocene: Bio-Chronological and Oceanographic Indicator. Geosciences (Basel) 12. https://doi.org/10.3390/geosciences12060244.

Marriner, N., Kaniewski, D., Pourkerman, M., Devillers, B., 2022. Anthropocene tipping point reverses long-term Holocene cooling of the Mediterranean Sea: a meta-analysis of the basin's Sea Surface Temperature records. Earth Sci. Rev. 227, 103986 https://doi.org/10.1016/j.earscirev.2022.103986.

Marullo, S., Artale, V., Santoleri, R., 2011. The SST multidecadal variability in the atlantic–mediterranean region and its relation to AMO. J. Climate 24, 4385–4401. https://doi.org/10.1175/2011JCLI3884.1.

MedECC, 2021. Climate and Environmental Change in the Mediterranean Basin – Current Situation and risks for the Future. First Mediterranean Assessment Report.

Menna, M., Poulain, P.-M., Ciani, D., Doglioli, A., Notarstefano, G., Gerin, R., Rio, M.-H., Santoleri, R., Gauci, A., Drago, A., 2019. New Insights of the Sicily Channel and Southern Tyrrhenian Sea Variability. Water (Basel). https://doi.org/10.3390/w11071355.

Morard, R., Füllberg, A., Brummer, G.-J.A., Greco, M., Jonkers, L., Wizemann, A., Weiner, A.K.M., Darling, K., Siccha, M., Ledevin, R., Kitazato, H., de Garidel-Thoron, T., de Vargas, C., Kucera, M., 2019. Genetic and morphological divergence in the warm-water planktonic foraminifera genus Globigerinoides. PloS One 14, e0225246. https://doi.org/10.1371/journal.pone.0225246.

Onken, R., 2003. Data-driven simulations of synoptic circulation and transports in the Tunisia-Sardinia-Sicily region. J. Geophys. Res. 108, 8123. https://doi.org/10.1029/2002JC001348.

Pallacks, S., Ziveri, P., Martrat, B., Mortyn, P.G., Grelaud, M., Schiebel, R., Incarbona, A., Garcia-Orellana, J., Anglada-Ortiz, G., 2021. Planktic foraminiferal changes in the western Mediterranean Anthropocene. Glob Planet Change 204, 103549. https://doi.org/10.1016/j.gloplacha.2021.103549.

Peeters, F.J.C., Brummer, G.-J.A., Ganssen, G., 2002. The effect of upwelling on the distribution and stable isotope composition of Globigerina bulloides and Globigerinoides ruber (planktic foraminifera) in modern surface waters of the NW Arabian Sea. Glob Planet Change 34, 269–291. https://doi.org/10.1016/S0921-8181(02)00120-0.

Peleg, O., Guy-Haim, T., Yeruham, E., Silverman, J., Rilov, G., 2020. Tropicalization may invert trophic state and carbon budget of shallow temperate rocky reefs. J. Ecol. 108, 844–854. https://doi.org/10.1111/1365-2745.13329.

Pinardi, N., Masetti, E., 2000. Variability of the large scale general circulation of the Mediterranean Sea from observations and modelling: a review. Palaeogeogr Palaeoclimatol Palaeoecol 158, 153–174. https://doi.org/10.1016/S0031-0182(00)00048-1.

POEM group, 1992. General-Circulation of the Eastern Mediterranean. Earth Sci Rev 32, 285–309.

Pujol, C., Vergnaud Grazzini, C., 1995. Distribution patterns of live planktic foraminifera as related to regional hydrography and productive system of the Mediterranean Sea. Mar Micropaleontol 25, 187–217.

Reimer, P.J., Bard, E., Bayliss, A., Beck, J.W., Blackwell, P.G., Ramsey, C.B., Buck, C.E., Cheng, H., Edwards, R.L., Friedrich, M., Grootes, P.M., Guilderson, T.P., Haflidason, H., Hajdas, I., Hatté, C., Heaton, T.J., Hoffmann, D.L., Hogg, A.G., Hughen, K.A., Kaiser, K.F., Kromer, B., Manning, S.W., Niu, M., Reimer, R.W., Richards, D.A., Scott, E.M., Southon, J.R., Staff, R.A., Turney, C.S.M., van der Plicht, J., 2013. IntCal13 and Marine13 Radiocarbon Age Calibration Curves 0–50,000 years cal BP. Radiocarbon 55, 1869–1887. https://doi.org/10.2458/azu_js_rc.55.16947.

Richey, J.N., Thirumalai, K., Khider, D., Reynolds, C.E., Partin, J.W., Quinn, T.M., 2019. Considerations for Globigerinoides ruber (White and Pink) Paleoceanography: Comprehensive Insights from a Long-running Sediment Trap. Paleoceanogr Paleoclimatol 34, 353–373. https://doi.org/10.1029/2018PA003417.

Rigual-Hernández, A.S., Sierro, F.J., Bárcena, M.A., Flores, J.A., Heussner, S., 2012. Seasonal and interannual changes of planktic foraminiferal fluxes in the Gulf of Lions (NW Mediterranean) and their implications for paleoceanographic studies: two 12-year sediment trap records. Deep-Sea Res. I Oceanogr. Res. Pap. 66, 26–40. https://doi.org/10.1016/j.dsr.2012.03.011.

Rinaldi, E., Nardelli, B.B., Volpe, G., Santoleri, R., 2014. Chlorophyll distribution and variability in the Sicily Channel (Mediterranean Sea) as seen by remote sensing data. Cont. Shelf Res. 77, 61–68. https://doi.org/10.1016/j.csr.2014.01.010.

Robinson, A.R., Golnaraghi, M., 1994. The physical and dynamical oceanography of the Mediterranean Sea. In: Ocean Processes in Climate Dynamics: Global and Mediterranean Examples, pp. 255–306. https://doi.org/10.1007/978-94-011-0870-6_12.

Robinson, A.R., Sellschopp, J., Warn-Varnas, A., Leslie, W.G., Lozano, C.J., Haley, P.J., Anderson, L.A., Lermusiaux, P.F.J., 1999. The Atlantic Ionian stream. J. Mar. Syst. 20, 129–156. https://doi.org/10.1016/S0924-7963(98)00079-7.

Rohling, E.J., Marino, G., Grant, K.M., 2015. Mediterranean climate and oceanography, and the periodic development of anoxic events (sapropels). Earth Sci Rev 143, 62–97. https://doi.org/10.1016/j.earscirev.2015.01.008.

Sabatier, P., Dezileau, L., Colin, C., Briqueu, L., Bouchette, F., Martinez, P., Siani, G., Raynal, O., Von Grafenstein, U., 2012. 7000years of paleostorm activity in the NW Mediterranean Sea in response to Holocene climate events. Quatern. Res. 77, 1–11. https://doi.org/10.1016/j.yqres.2011.09.002.

Salgado-Hernanz, P.M., Regaudie-de-Gioux, A., Antoine, D., Basterretxea, G., 2022. Pelagic primary production in the coastal Mediterranean Sea: variability, trends, and contribution to basin-scale budgets. Biogeosciences 19, 47–69. https://doi.org/10.5194/bg-19-47-2022.

Sarmiento, J.L., Herbert, T.D., Toggweiler, J.R., 1988. Causes of anoxia in the world ocean. Global Biogeochem. Cycles. https://doi.org/10.1029/GB002i002p00115.

Schiebel, R., Hemleben, C., 2005. Modern planktic foraminifera. Palaontol Z 79, 135–148. https://doi.org/10.1007/BF03021758.

Schiebel, R., Hemleben, C., 2017. Planktic Foraminifers in the Modern Ocean. Springer-Verlag, Berlin, Heidelberg. https://doi.org/10.1007/978-3-662-50297-6.

Schmuker, B., Schiebel, R., 2002. Planktic foraminifers and hydrography of the eastern and northern Caribbean Sea. Mar. Micropaleontol. 46, 387–403. https://doi.org/10.1016/S0377-8398(02)00082-8.

Seears, H.A., Darling, K.F., Wade, C.M., 2012. Ecological partitioning and diversity in tropical planktonic foraminifera. BMC Evol. Biol. 12, 54. https://doi.org/10.1186/1471-2148-12-54.

Spezzaferri, S., Kucera, M., Pearson, P.N., Wade, B.S., Rappo, S., Poole, C.R., Morard, R., Stalder, C., 2015. Fossil and genetic evidence for the polyphyletic nature of the planktonic foraminifera "globigerinoides, and description of the new genus trilobatus. PloS One 10, e0128108. https://doi.org/10.1371/journal.pone.0128108.

Sprovieri, R., Di Stefano, E., Incarbona, A., Gargano, M.E., 2003. A high-resolution record of the last deglaciation in the Sicily Channel based on foraminifera and calcareous nannofossil quantitative distribution. Palaeogeogr. Palaeoclimatol. Palaeoecol. 202, 119–142. https://doi.org/10.1016/S0031-0182(03)00632-1.

Sprovieri, R., Di Stefano, E., Incarbona, A., Oppo, D.W., 2006. Suborbital climate variability during Marine Isotopic Stage 5 in the Central Mediterranean basin: evidence from calcareous plankton record. Quat. Sci. Rev. 25 https://doi.org/10.1016/j.quascirev.2006.01.035.

Steinhilber, F., Beer, J., Fröhlich, C., 2009. Total solar irradiance during the Holocene. Geophys. Res. Lett. 36 https://doi.org/10.1029/2009GL040142.

Trenberth, K.E., Shea, D.J., 2006. Atlantic hurricanes and natural variability in 2005. Geophys. Res. Lett. 33 https://doi.org/10.1029/2006GL026894.

Vallefuoco, M., Lirer, F., Ferraro, L., Pelosi, N., Capotondi, L., Sprovieri, M., Incarbona, A., 2012. Climatic variability and anthropogenic signatures in the Gulf of Salerno (southern-eastern Tyrrhenian Sea) during the last half millennium. Rendiconti Lincei 23, 13–23. https://doi.org/10.1007/s12210-011-0154-0.

Zampieri, M., Toreti, A., Schindler, A., Scoccimarro, E., Gualdi, S., 2017. Atlantic multi-decadal oscillation influence on weather regimes over Europe and the Mediterranean in spring and summer. Glob Planet Change 151, 92–100. https://doi.org/10.1016/j.gloplacha.2016.08.014.

Žarić, S., Donner, B., Fischer, G., Mulitza, S., Wefer, G., 2005. Sensitivity of planktic foraminifera to sea surface temperature and export production as derived from sediment trap data. Mar Micropaleontol 55, 75–105. https://doi.org/10.1016/j.marmicro.2005.01.002.

Zarkogiannis, S., Kontakiotis, G., Antonarakou, A., 2020. Recent planktonic foraminifera population and size response to Eastern Mediterranean hydrography. Rev. Micropaleontol. 69, 100450 https://doi.org/10.1016/j.revmic.2020.100450.